Numerical simulation of residual thermal stresses in AA7050 alloy during DC-casting using ALSIM5

M. Lalpoor[1,a], D. Eskin[1,b] and L. Katgerman[2,c]

[1]Materials innovation institute, Mekelweg 2, 2628CD Delft, The Netherlands

[2]Delft University of Technology, Department of Materials Science and Engineering, Mekelweg 2, 2628CD Delft, The Netherlands

[a]M.Lalpoor@tudelft.nl, [b]D.G.Eskin@tudelft.nl,[c]L.Katgerman@tudelft.nl

Keywords: DC-casting, Thermo mechanical simulation, Residual thermal stresses, Cold cracking.

Abstract. Non-homogenous cooling rates and solidification conditions during DC-casting of high strength aluminum alloys result in the formation and accumulation of residual thermal stresses with different signs and magnitudes in different locations of the billet. Rapid propagation of micro-cracks in the presence of thermal stresses can lead to catastrophic failure in the solid state, which is called *cold cracking*. Numerical models can simulate the thermomechanical behavior of an ingot during casting and after solidification and reveal the critical cooling conditions that result in catastrophic failure, provided that the constitutive parameters of the material represent genuine as-cast properties. Simulation of residual thermal stresses of an AA7050 alloy during DC-casting by means of ALSIM5 showed that in the steady-state conditions large compressive stresses formed near the surface of the billet in the circumferential direction. Stresses changed sign on moving towards the centre of the billet and became tensile with high magnitudes in radial and transverse directions, which made the alloy prone to hot and cold cracking.

Introduction

7xxx series aluminum alloys are widely used in aircraft industry mainly because of their high strength to weight ratio. They owe such admirable mechanical properties to special age hardening treatments performed after deformation, hence not in the as-cast condition. Low thermal conductivity values compared to other aluminum alloys result in high temperature gradients, which in turn leads to accumulation of thermal stresses with different signs and magnitudes in different locations of the billets during DC-casting. Presence of non-equilibrium phases especially on grain boundaries and in inter-dendritic spaces provides favorable paths for the crack initiation and propagation, and makes the material prone to cold cracking.

Numerical simulation of thermal stresses during DC-casting of these alloys can reveal those stages and locations at which the material's susceptibility to cracking is high. Some researchers have performed such simulations using different commercial and non-commercial finite element packages and have derived the state of stresses and strains resulted from corresponding temperature gradients [1-5]. Even some cracking criteria have been derived by applying the fracture mechanics to the normal stresses gained from simulations to predict cracking and catastrophic failure in the completely solid state, i.e. "cold cracking" [6,7]. The main problem is, however, that the derived criteria can only be realistic providing that the mechanical properties and constitutive parameters used for the determination of simulation results are extracted from the samples in the genuine as-cast condition. In the homogenized or stress relieved states the material shows higher plasticity [8,9] and the constitutive parameters are different, which can lead to unreliable simulated stress and strain levels in the billet. In this research work the finite element package ALSIM5 has been used to compute temperatures, thermal stresses, and strains during the starting phase and the steady-state regime in an aluminum 7050 alloy billet. An elasto-viscoplastic model [10] was applied which assumes the strong temperature dependence of the constitutive and mechanical properties in the as-

cast condition. The constitutive parameters were gained from room- and high-temperature tensile tests of the material in the as-cast condition.

Presentation of the Model

As mentioned in the previous section, ALSIM5 was used for the computation of temperature profile and stress/strain fields in the round AA7050 billet. The description of the model can be found elsewhere [11-14]. Geometry of the setup consisted of hot top, mould, water jet, bottom block, and the cast domain. New elements with the size of 0.75 mm are added to the geometry at the casting speed to simulate the continuous casting conditions. So during the casting, the bottom block moves downwards while new elements are added to the system, and the mould, hot top and molten metal preserve their initial position. Due to axial symmetry, only half of the billet is considered. Time-dependent thermal boundary conditions are defined to account for filling time, the air gap formation between the billet and the bottom block as well as at the billet surface, and for different heat extraction in different parts of the casting system [10]. The process parameters are mentioned in Table 1.

Table1. Description of casting process parameters.

Process parameter	Value
Ingot radius [mm]	100
Final length of the billet [mm]	500
Casting speed [mm/min]	60
Melt temperature [ºC]	680
Water flow rate [l/min]	80
Water temperature [ºC]	15
Start temperature of bottom block [ºC]	20

Table 2. Constitutive parameters of the 7050 alloy determined from the extended Ludwik equation.

Temp. [ºC]	K [MPa]	n	m	E [GPa]	Poisson's ratio
20	774 ± 32	0.42 ± 0.02	0	67.9	0.338
100	626 ± 13	0.38 ± 0.01	0	64.9	0.341
200	392 ± 11	0.21 ± 0.006	0	61.2	0.346
300	199 ± 4.5	0.11 ± 0.007	0.03 ± 0.007	57.4	0.352
400	174 ± 5	0.09 ± 0.01	0.15 ± 0.009	53.6	0.358

Thermal Properties. Thermal as well as fluid properties of the alloy were gained from the thermodynamics database JMat-Pro provided by Corus-Netherlands (IJmuiden). The temperature dependence of the coefficient of thermal expansion, specific heat, heat conductivity, fraction solid density and kinematic viscosity were extracted and embedded in the model. Solidification range as well as liquidus and non-equilibrium solidus were determined using DSC tests.

Mechanical Properties. Tensile mechanical properties of as-cast 7050 samples were measured by authors in a Gleeble-1500 thermomechanical simulator and the details are described elsewhere [15]. In order to simulate the cooling of the billet from solidus temperature to room temperature the extended Ludwik equation was applied:

$$\sigma = K(\mathrm{T})(\varepsilon_p + \varepsilon_p^0)^{n(T)}(\dot{\varepsilon}_p)^{m(T)}, \quad (1)$$

where K(T) is the consistency of the alloy, n(T) is the strain hardening coefficient, m(T) is the strain rate sensitivity, and ε_p^0 is a constant equal to 0.001 [16]. Values of K(T), n(T) and m(T) (Table 2) were embedded in the model using the ALSPEN fitting functions [10], where n, m and K are nonlinear functions of T. An onset temperature T_0, above which the strain hardening can be neglected, was determined to be 663 K. Above this temperature ALSPEN equations and cohesion

model [17] are combined. Poisson's ratio values were gained from JMat-Pro and the Young's modulus values were obtained from rheological torsion tests using an RMS-800 setup.

Results and Discussion

Casting simulation was performed for 500 sec (casting length of 500 mm) to make sure that the steady-state conditions are gained and stress analysis can be done. From this moment onwards the stresses remain more or less unchanged till changes in the thermal boundary conditions were applied or casting ceased. The lower part of the billet has reached temperatures below 80 ºC. Figures 1(a) through (d) show the contour maps of the four components of thermal stresses generated under steady-state casting conditions. As can be seen the residual radial stresses, displayed in the lower part of the billet (on the top of the bottom block) is compressive, which turns to tensile as we move in the positive "y" direction. Along the radial axis (x-axis) radial thermal stresses change sign from tensile (maximum 70 MPa) to compressive (minimum -8 MPa) as we move to the surface. Similar trend is observed for the circumferential component of the residual stress, but its compressive component is much larger in the vicinity of the surface (Fig. 1b). Contour map of axial thermal stresses (along "z" axis) follows the same trend in the lower part of the billet. This changes in the upper part of the billet where we see compressive stresses below the high temperature zone of the billet and tensile stresses around the water impingement area (Fig. 1c). Shear stress components are mainly negative with largest values around the water impingement area and in the lower part of the billet in the vicinity of the bottom block (Fig. 1d). Eventually it can be seen that the water impingement below the mold has a considerable effect on the final induced stress state, especially the circumferential component.

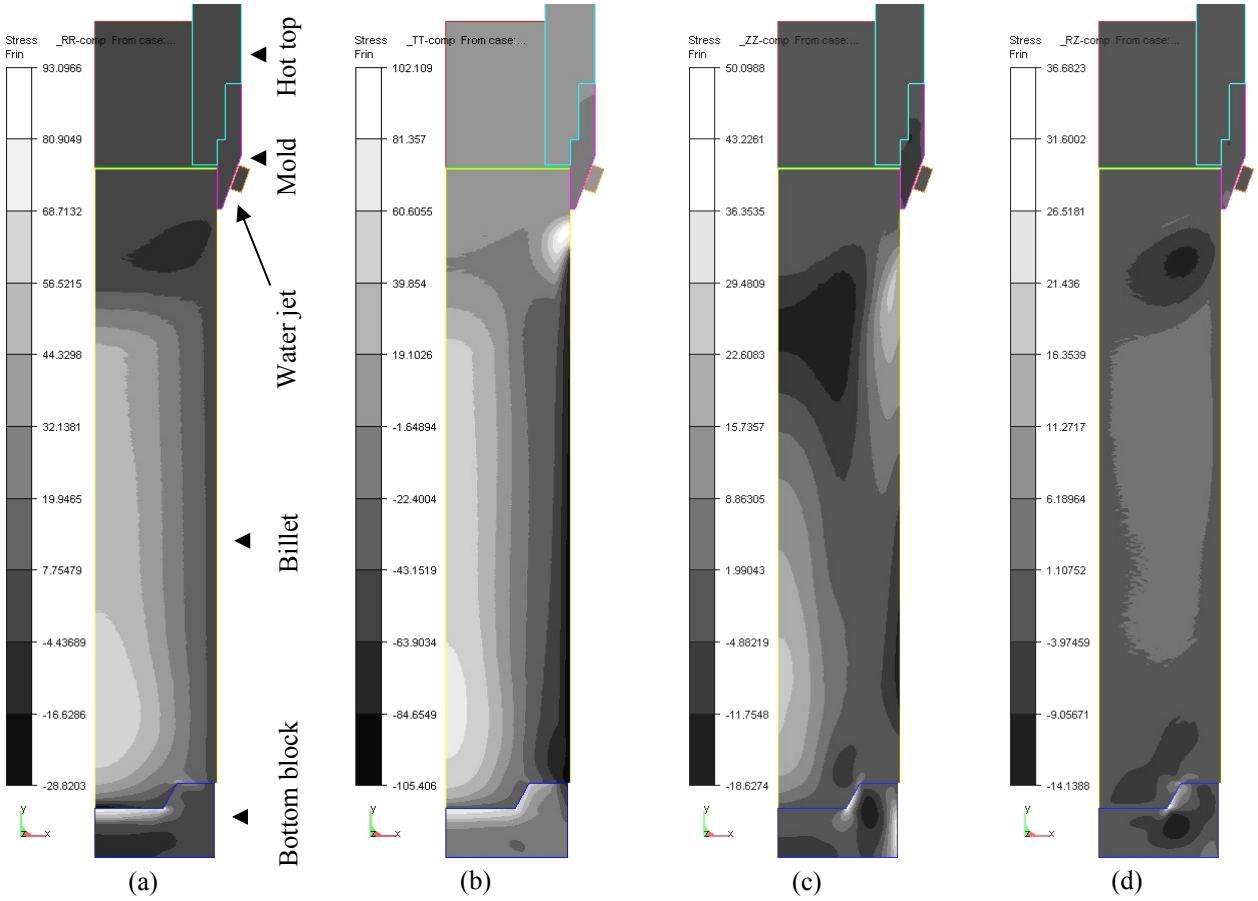

Fig. 1 Thermal stresses in steady-state conditions after 500 sec: (a) radial, b) circumferential, c) axial, and d) shear component.

Contour maps of the viscoplastic part of the strain are shown in Fig. 2(a) through (d). The radial component of the strain is mostly tensile in the lower central part of the billet, decreases in mid-radius and increases again as we move to the surface of the billet. In the upper parts of the billet it remains homogenous and relatively low in value, except for the surface of the billet. The circumferential component (Fig 2(b)) appears to be tensile in the bottom center of the billet and by moving to the surface it turns to compressive values in the lower corner. Unlike radial and circumferential components, the axial component of the strain shows negative (compressive) values in the center (with a min. on top of the bottom block) and by moving to the surface (except for upper part) it converts to tensile (Fig2(c)). The compressive values of the axial strains in the lower part of the billet seem to be unexpected compared to the axial stress component. But this is mainly the consequence of compressive axial viscoplastic strain rate near the solidification front as explained by Fjaer et *al.* [10], and of course the lateral contraction caused by larger tensile values of the radial and circumferential components of the stress tensor.

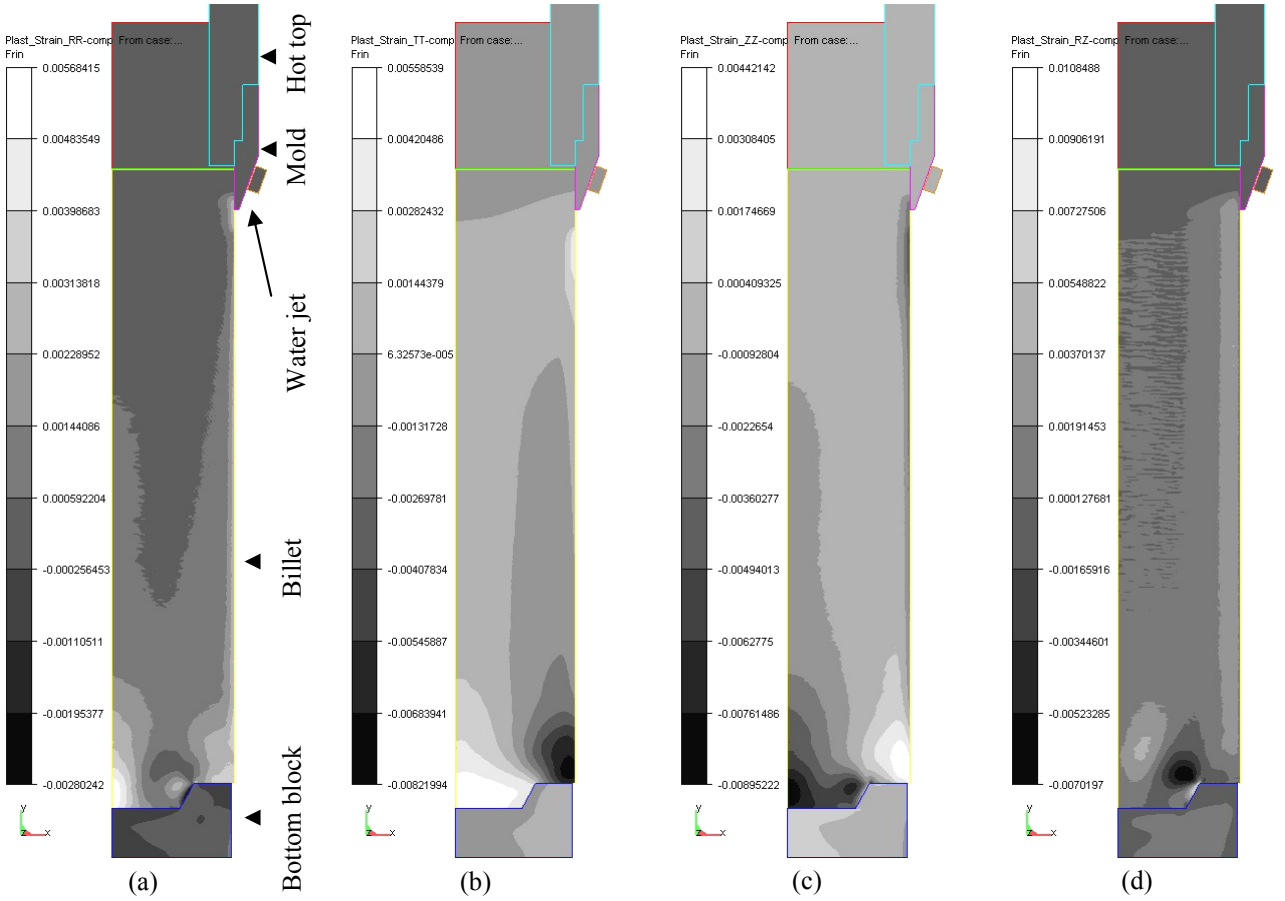

Fig. 2 Viscoplastic strain at steady-state conditions after 500 sec: (a) radial, b) circumferential, c) axial, and d) shear components.

In order to examine the occurrence of plastic yield in the billet, contour maps of the temperature, the hardening parameter α ($\alpha = \int d\alpha,\ \alpha = \begin{cases} d\bar{\varepsilon}_p & \text{when } T \le T_0 \\ 0 & \text{otherwise} \end{cases}$) and effective stress are used (Figs 3(a) to 3(c)). In those locations of the billet where the temperature is above T_0 or no yielding is present (α=0) the total viscoplastic strain is generated by creep, which is the case for almost the whole billet (Fig. 3(b)). A result of strain hardening can be seen in Fig. 3(c), where the effective stress at the surface is greater than 100 [MPa], which is certainly above the 0.2% offset yield strength of the 7050 alloy above 200 ºC [18]. The maximum value of the effective viscoplastic strain appeared to be 1.2% and was observed mainly in the surface of the billet and in the lowest central part on top of the bottom block (contours not shown here).

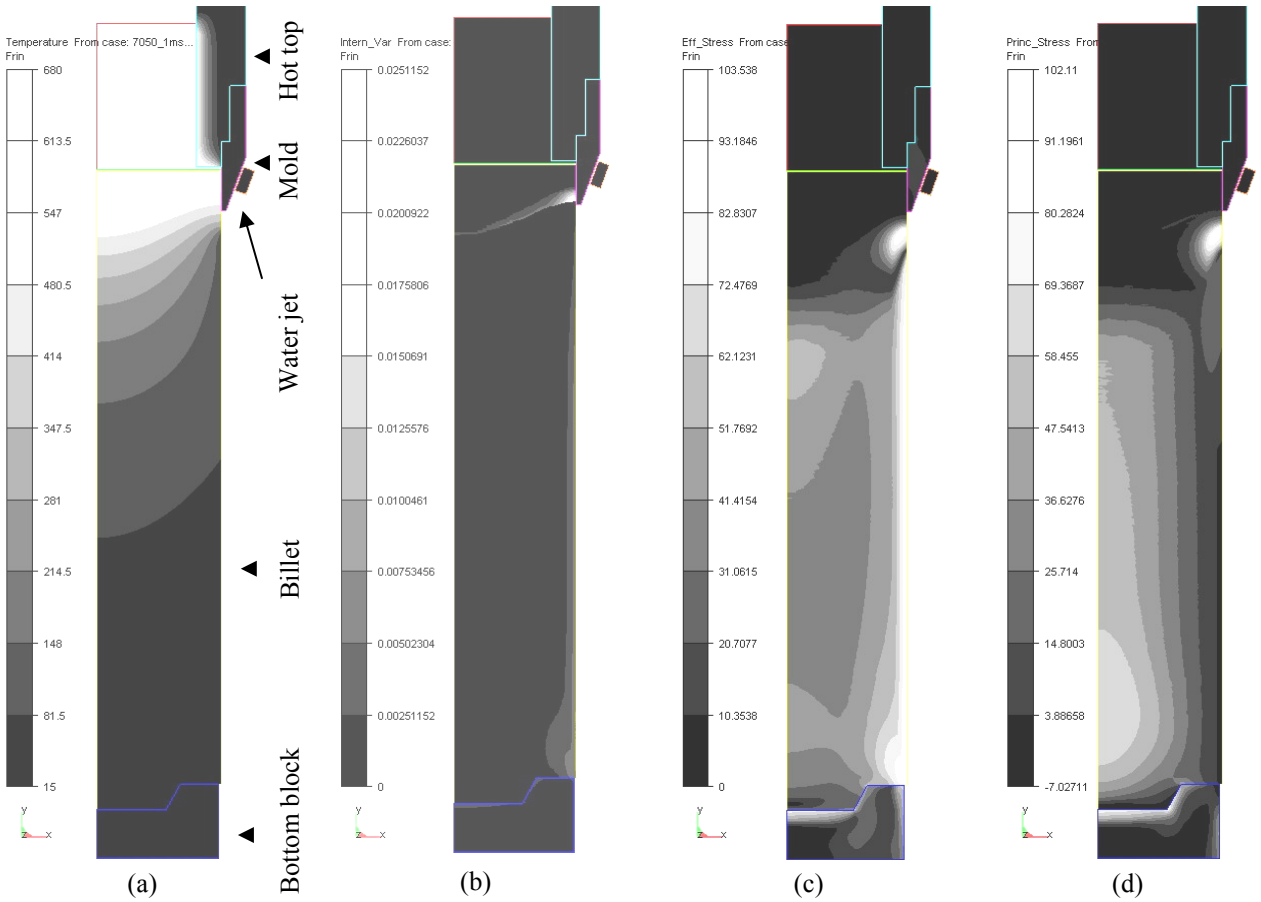

Fig. 3 Investigation of plastic yield and strain hardening using: (a) temperature profile, b) hardening parameter, c) effective stress, and d) the largest component of the principle stresses.

Effective stress or hardening parameter contours provide us with useful information on yielding of the material. The largest component of the principle stresses on the other hand can be used to asses the locations where the billet is more prone to cracking (Fig. 3(d)). The maximum value of the tensile principle stress appears after 215 seconds of casting in the center of the billet, where the temperature is around 200ºC. From this moment on, this component of stress remains roughly constant and accounts for the cracks formed in the center of the 7050 DC-cast billets. Principle stresses are all compressive in the surface of the billet, except for the water impingement zone, where they are highly tensile.

Conclusions

Computation of the residual thermal stresses in a 7050 billet during DC-casting revealed that these stresses appear to be mainly tensile in the center of the billet and by moving to the surface of the billet they change to compressive with high magnitude in circumferential direction. Tensile nature of the radial, axial and circumferential components of the stress tensor in the center of the billet accounts for the highest probability of crack initiation and propagation in this region. Crack initiation can occur by hot cracking in the semi-solid region or cold cracking in the completely solid alloy where the yield strength is still low. This has been experimentally proved by observation of cracks in the center of the 7050 billets (few millimeters long). Gradual propagation of such cracks up to critical length and catastrophic failure takes place later on when the ductility of the material suddenly falls at temperatures below 300 ºC [18]. The water impingement zone simultaneously generates high tensile principle stress components, which can also facilitate the formation of micro-cracks in this area. Initiated cracks can later on propagate when the magnitude of the compressive

circumferential stress decreases at the end of casting. Viscoplastic strains in the center of the billet are mainly caused by creep at high temperatures, whereas, at the surface and near the solidification front a high hardening parameter (α) is observed that accounts for plastic deformation in those areas.

Acknowledgments

This research was carried out under the project number 05237 in the framework of the Research Program of the Materials innovation institute (www.m2i.nl), former Netherlands Institute for Metals Research. Support and fruitful discussions with Dr. W. Boender (Corus R&D) are appreciated. Another important basis of the present paper is comments received from Mr. D. Mortensen, Mr. H. Fjaer and Dr. A. Ten Cate. Authors would like to especially thank Dr. A. Ten Cate for the preparation of the geometry and mesh simulation files.

References

[1] B. Hannart, F. Ciaalti and R. van Schalkwijk, in: Light Metals, edited by U. Mannweiler, TMS (1994), pp. 879-887.
[2] Drezet J.M. and M. Rappaz, in: Light Metals, edited by J. Evans, TMS (1995), pp. 941-950.
[3] Keh-Minn Chang, B. Kang: Journal of Chinese Institute of Engineers, Vol. 22 (1999), No.1, pp. 27-42.
[4] H.G. Fjaer, A. Mo, in: Light Metals, edited by C.M. Bickert, TMS (1990), pp. 945-950.
[5] W. Boender, A. Burghardt, E.P. van Klaveren, and J. Rabenberg, in: Light Metals, edited by A.T. Tabereaux, TMS (2004), pp. 679-684.
[6] O. Ludwig, J.-M. Drezet, B. Commet, B. Heinrich, in: Modeling of Casting, Welding and Advanced Solidification Processes, edited by C-A. Gandin and M. Bellet, TMS (2006), pp.185-192.
[7] W. Boender, A. Burghardt, in: 5th Decennial Int. Conf. on Solidification Processing, edited by H. Jones, Sheffield, UK, 2007, pp. 714-718.
[8] J. Wan, H.M. Lu, K. M. Chang, J. Harris, in: Light Metals, edited by B. Welch, TMS (1998), pp. 1065-1071.
[9] K.-M. Chang, H.-M. Lu, J. Wan, in: Second Intern. Conf. on Quenching and Control of Diffusion, edited by J.F. Harris, ASM International (1996), pp. 341–345.
[10] H.G. Fjaer, A. Mo, Metallurgical Transactions B, Vol. 21-B (1990), pp. 1049-1061.
[11] E.E. Madsen and G.E. Fladmark, in: Numerical Solution of Partial Differential Equations, edited by G.E. Fladmark and J.G. Gram, D. Reidel Publishing Company, Dordrecht, The Netherlands (1973), pp.223-40.
[12] E.E. Madsen, in: Numerical Methods in Thermal Problems, edited by R.W. Lewis and K. Morgan, Pineridge Press Limited, Swansea, United Kingdom (1979), pp. 81-89.
[13] H. Fossheim and E.E. Madsen, in: Light Metals, edited by W.S. Peterson, TMS-AIME (1979), pp. 695-720.
[14] E.K. Jensen and W. Schneider, in: Light Metals, edited by Christian M. Bickert, TMS-AIME (1990), pp. 937-43.
[15] M. Lalpoor, D. Eskin, and L. Katgerman: submitted to 12th International Conference on Fracture, Ottawa, Canada, 2009.
[16] B. Magnin, L. Katgerman, B. Hannart, in: Modeling of Casting, Welding and Solidification Process, edited by M. Cross and J. Campbell, Warrendale, USA (1995), pp. 303-310.
[17] C.L. Martin, O. Ludwig and M.Suéry, in: Aluminum Alloys: Their Physical and Mechanical Properties, edited by P.J. Gregson and S.J. Harris, Mater. Sci. Forum, Vol. 396-402 (2002), pp. 265-270.
[18] M. Lalpoor, D. Eskin, and L. Katgerman: Mater. Sci. Eng. A Vol. 497 (2008), pp. 186-194.